

## TRANSFORMATION DEPENDENCE OF PZT AS SHOWN BY PFM

S Dunn and R W Whatmore

Transformation dependence of lead zirconate titanate (PZT) as shown by PiezoAFM surface mapping of Sol-gel produced PZT on various substrates.

S. Dunn and R. W. Whatmore

Building 70, Nanotechnology, Cranfield University, Cranfield, MK43 0AL, UK

### **Abstract**

PZT was grown on STP (Si/SiO<sub>2</sub>/Ti/Pt (Ti 5nm, Pt 100nm)), SAP (Si/Si<sub>3</sub>N<sub>4</sub>/Al/Ti/Pt (Al 100nm, Ti 10nm, Pt 15nm)) and GI (Glass/ITO(Indium Tin Oxide)). In each case the PZT underwent the same heat treatment, 200°C for 2 minutes and then 530°C for 5 minutes. The extent of perovskite formation was evaluated using Piezoresponse force microscopy (PFM). This provided information about the domain orientation and spatial distribution of ferroelectric material in the PZT film. This showed that PZT/STP underwent complete transformation to the perovskite phase. However, for the PZT/SAP and GI incomplete transformation to the perovskite occurred. A system of rosettes surrounded by an amorphous matrix developed. The size and density of the PZT rosettes on the surface was found to be substrate dependent. For Gi/PZT the density of rosettes formation is ca. 1/μm<sup>2</sup>, compared to 4/μm<sup>2</sup> for PZT/SAP. The rosettes for the PZT on GI grow a maximum size of 2μm, which compares to 1μm for PZT on SAP. Differences in the observed growth rate and nucleation density are associated with the back electrode stability and crystal structure, effects that will be discussed in this paper.

KEYWORDS: piezoresponse force microscopy, nucleation, PZT, ferroelectric domains

### **Introduction**

Ferroelectric materials such as lead zirconate titanate (PZT PbZr<sub>x</sub>Ti<sub>1-x</sub>O<sub>3</sub>) have been undergoing increasing study in recent years, as their suitability for use in non-volatile memories and other MEMS applications has been recognised<sup>1,2,3</sup>. The development of techniques, such as sol-gel, that allow the production of very highly orientated thin film PZT at temperatures compatible with standard Si fabrication techniques has further enhanced this interest<sup>4,5</sup>. For devices to be made successfully the ferroelectric material produced should be high quality with a minimum of rosettes and for many applications highly [111] orientated.

# TRANSFORMATION DEPENDENCE OF PZT AS SHOWN BY PFM

S Dunn and R W Whatmore

The scale of interest for the grain and domain structures is now sub-micron. Standard analytical techniques do not allow the determination of ferroelectric properties at this scale. The development of atomic force microscopy has allowed the routine evaluation of surface topography of these materials, and in the last few years a number of additional techniques have been developed. Prime among these for determining the ferroelectric properties of material is piezoelectric atomic force microscopy (P-AFM). P-AFM detects the converse piezoelectric response of the material under investigation and allows the mapping of the ferroelectric domains. The use of an AFM tip as a small and moveable conductive probe has reduced the scale of the study of piezoelectricity to just a few tens of nanometers. Using piezoresponse force microscopy (PFM) it is possible to map ferroelectric domains in a film without a top electrode and without altering them<sup>6,7,8</sup>.

## **Experimental**

A schematic of the experimental arrangement used to perform PFM is shown in Figure 1. A sinusoidal signal was passed between the AFM tip, a nanosensors tapping mode tip made from doped Si with a resonant frequency of ca 280,000 Hz, and the back electrode of the PZT sample, usually held at ground. The signal used in all cases was 18kHz and 2V peak-peak. The resonant frequency chosen was well below the fundamental resonant frequency for the cantilever and 2 V p-p was below the coercive field for the samples under evaluation. The converse piezoelectric effect causes a distortion in the shape of the sample due to the external electric field. When completing PFM, a lock-in amplifier is used to filter the distortions due to the converse piezoelectric effect from the bulk topographic signal. In this way it is possible to obtain both topographical and piezoelectric data in one experimental run.

It has also been shown that when a field in excess of the coercive field is applied between the AFM tip and ground the material in that region is poled<sup>9,10</sup>. Using this technique it is possible to manipulate the domain structure in the ferroelectric material. By applying a DC bias in series with the AC signal passed between the tip and ground, it is possible to produce hysteresis loops from localised regions of the material<sup>11,12</sup>. In this paper we use the term  $\delta_{33}$  to describe the response of the ferroelectric film under investigation.

Films of 210nm were prepared using a sol-gel technique that has been described in earlier work<sup>4</sup>. The films were fired at two temperatures, initially, a pyrolysis temperature of 200°C and then a final phase transformation temperature of 520°C.

# TRANSFORMATION DEPENDENCE OF PZT AS SHOWN BY PFM

S Dunn and R W Whatmore

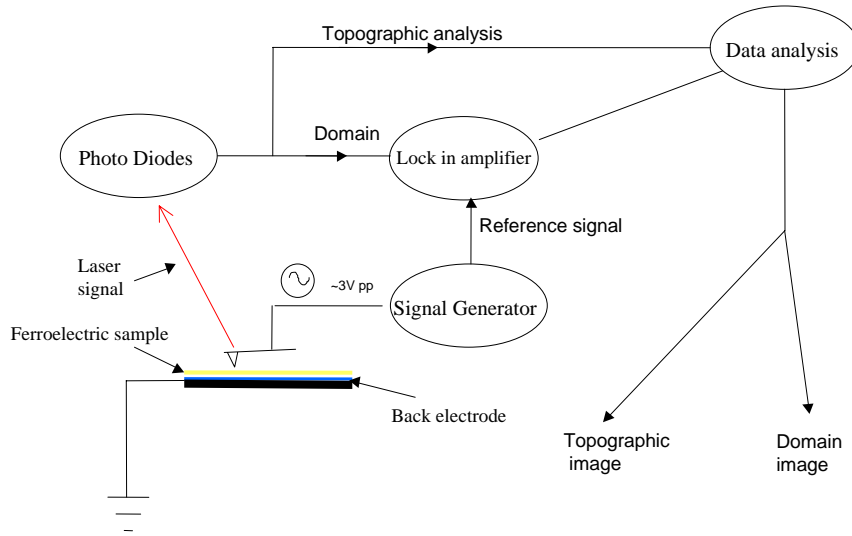


Figure 1: Schematic of P-AFM experimental arrangement.

A Siemens D5005 system using Bragg-Brentano geometry and  $\text{Cu } \alpha$  radiation was used to perform XRD analysis of the samples.

## **Results and Discussion**

### Topography

Samples of lead zirconate titanate PZT(30/70) deposited on Pt/Ti/SiO<sub>2</sub>/Si (STP), Pt/Ti/Al/Si<sub>3</sub>N<sub>4</sub>/Si (SAP) and Glass/ITO (GI) were examined using tapping mode AFM. Figure 2, shows the topography for a sample of PZT/SAP, the development of the rosettes in the film is clearly seen. The z-range for the image is 58nm, which is high when compared an average z-range of 20nm for PZT on STP. A typical topographic image for the surface of PZT in STP is shown in Figure 3. The image consists of a number of small, sub 100nm grains of PZT within some large surface features. The z-range for the image in Figure 3 is 23nm. An image of the surface of PZT on GI is shown in Figure 4. The surface shows a number of well defined rosettes and exhibits a z-range of 38nm.

### Piezoresponse force microscopy (PFM)

PFM studies have revealed that the domain structure in the as deposited films varies depending on the substrate used. The differences stem from the mechanism of perovskite formation from the non-ferroelectric pyrochlore phase. The PFM map for the surface of PZT-SAP is shown in Figure 5. The centre of the image has had

# TRANSFORMATION DEPENDENCE OF PZT AS SHOWN BY PFM

S Dunn and R W Whatmore

a positive bias (relative to tip) of 25V applied, and is shown by the boxed region. The area outside the box is the as deposited film. In the as deposited film it is difficult to differentiate between the regions of rosette and un-transformed pyrochlore. This indicates that the perovskite region of the film contains domains that are randomly orientated up or down.

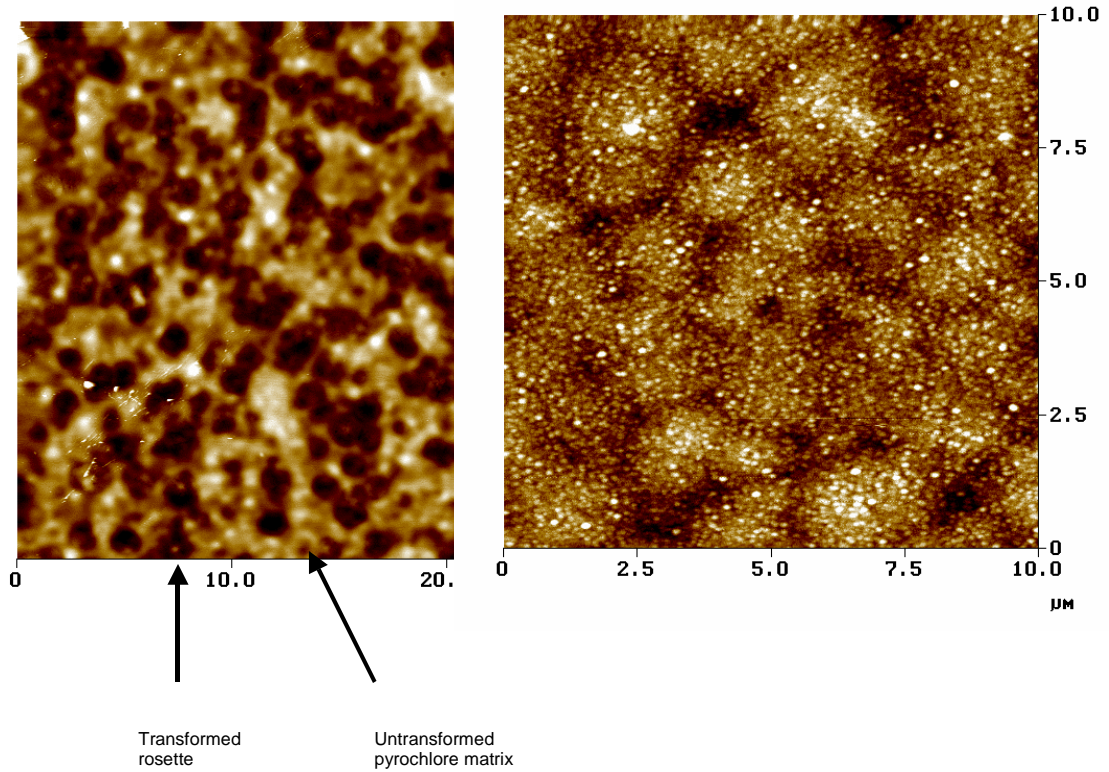


Figure 2: Topographic image of PZT grown on SAP obtained by Tapping Mode™ AFM. The maximum Z-range in the image is 58nm. The rosettes formed during nucleation of the perovskite phase are clearly shown in the image.

Figure 3: Topographic image of PZT grown on STP obtained by Tapping Mode™ AFM. The maximum Z-range in the image is 23nm. The grains of PZT are less than 100nm and are within a longer range ordering of the film. The film has completely transformed to the perovskite phase.

The region that has been subjected to a bias of +25V shows a series of bright white spots where the transformed perovskite rosettes are. The homogeneity of

## TRANSFORMATION DEPENDENCE OF PZT AS SHOWN BY PFM

S Dunn and R W Whatmore

these spots, the fact that they are all bright white is a consequence of the orientated nature of the film. The film is orientated in the [100] and [110] plane with respect to the substrate, explaining why there are two distinct levels of rosette brightness. It appears that each rosette has grown with the same crystallographic orientation, confirmed by the level of brightness being similar within rosettes. A high resolution image of the poled region of PZT on SAP is shown in Figure 6. The two different intensities of piezoresponse are shown very clearly in this image.

The PFM image obtained for PZT on GI is very different from that obtained for PZT on SAP. The PZT that grows on GI has been shown to have a powder XRD pattern. The PFM image shown in Figure 7 shows that the domain structure of the material varies within a rosette, unlike that of PZT/SAP. Another feature of the random orientation of PZT that grows on GI is that it is not possible to completely pole a given region. This is a direct result of the random orientation of the PZT in

the film, Figure 8 shows the effects of poling a region of PZT grown on GI. The image shown is for a sample of PZT that underwent special heat treatment.

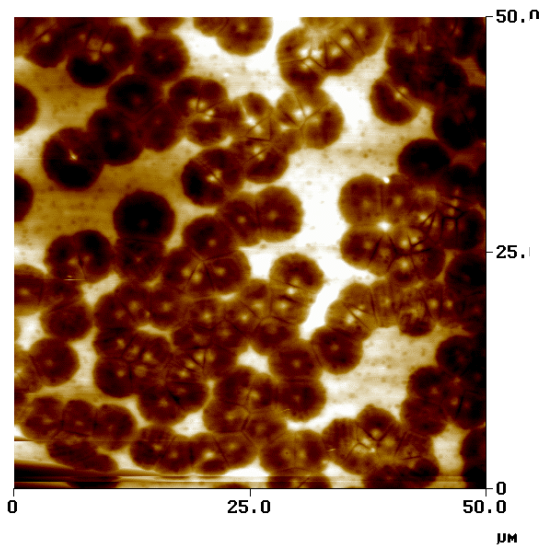


Figure 4: Topographic image of PZT grown on GI obtained by Tapping Mode™ AFM. The maximum Z-range in the image is 38nm, with the rosettes formed during perovskite nucleation being clearly defined.

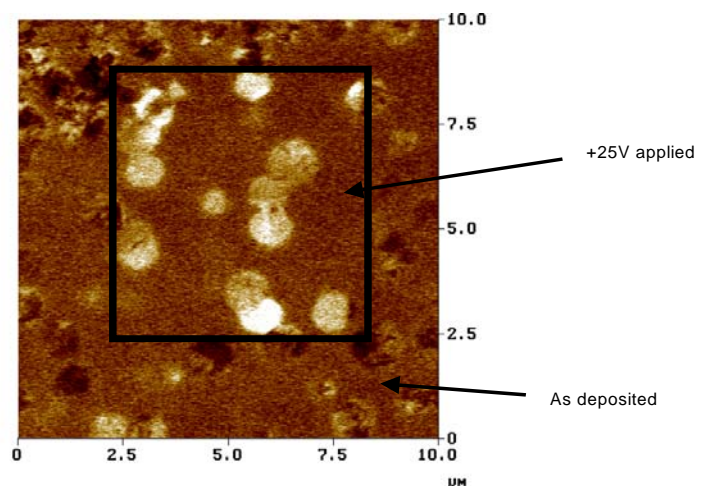


Figure 5: PFM map of the surface of PZT on SAP. The outer region is the as deposited region of the film, the boxed area in the centre has been poled by the application of +25V. The rosettes in the central region have been homogeneously poled which is a result of the crystallographic orientation of the film.

## TRANSFORMATION DEPENDENCE OF PZT AS SHOWN BY PFM

S Dunn and R W Whatmore

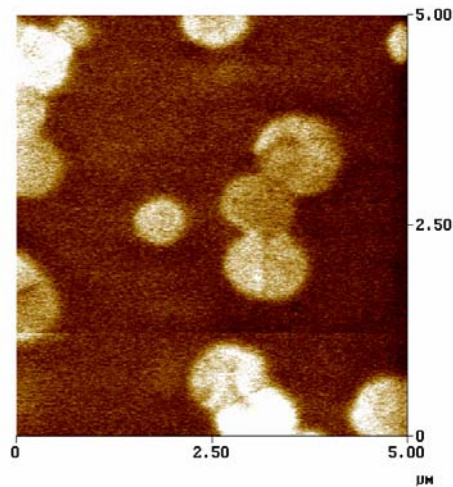


Figure 6: A high resolution P-AFM image of the poled region of PZT on SAP. The two intensities of response for the poled perovskite region are clearly seen.

The PFM image of PZT that grows on STP is quite different from both the cases above and is shown in Figure 9. The domain structure appears to be neutral as the response is grey. This indicates that the domains in the film are randomly orientated up or down, and that the size of the domains are not resolvable by the AFM at the scan size used. The film produced is very highly [111] orientated and so it is expected that it will be possible to pole regions and they will show as white or black regions. This has been demonstrated<sup>13</sup>.

The differences in the observed microstructure and PFM maps for the samples tested stems from the differences in the nucleation mechanisms for the development of the perovskite phase. The production of a ferroelectric thin film by the metal-organic route consists of a number of steps. In the case of the production of perovskite (piezoelectric) PZT, the sol is first pyrolysed, this forms the non-piezoelectric pyrochlore phase, this is then transformed by high temperature annealing into the piezoelectric perovskite phase. The transformation from pyrochlore to perovskite is dependent on a number of factors and of high significance is the density of suitable sites for the nucleation of the perovskite phase at the PZT-electrode interface.

In the case of PZT that is grown on a Pt back electrode then nucleation occurs due to interaction with the crystal lattice of the Pt and nucleating perovskite. Recently evidence has been found that shows that the formation of a Pt<sub>3</sub>Pb transient intermetallic phase also reduces the activation energy for perovskite formation<sup>14</sup>. The very highly orientated film of PZT grown on the surface of STP is a result of the close lattice match between the perovskite phase, the stability of the

## TRANSFORMATION DEPENDENCE OF PZT AS SHOWN BY PFM

S Dunn and R W Whatmore

intermetallic during phase transformation and the smooth surface of the Pt. In the SAP case the surface of the Pt electrode is very rough, exhibiting a series of peaks and troughs. Although the Pt on this surface is [111] orientated there is also evidence for the production of  $\text{AlPt}_2$ . The presence of the  $\text{AlPt}_2$  is likely to have a detrimental effect of the formation of the  $\text{Pt}_3\text{Pb}$  intermetallic and will increase the activation energy for perovskite formation. However, this does not fully explain the presence of the rosette structure, which would not be present if the perovskite was transforming on the crystal lattice of the Pt. It is thought that the rough nature of the Pt surface is preventing direct nucleation from the Pt crystal lattice. Nucleation of the perovskite phase occurs at discrete regions of the electrode surface and then progresses with an associated increase in the rosette size.

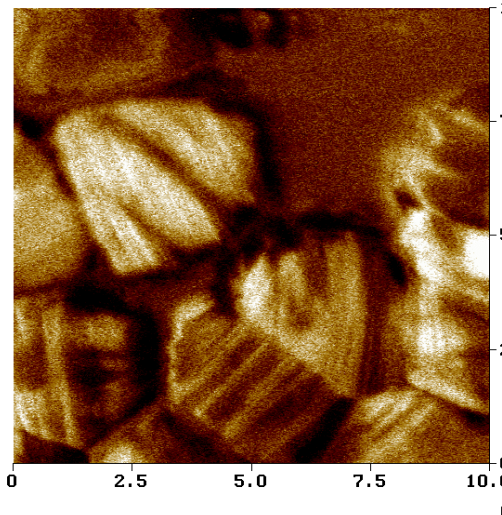


Figure 7: PFM image of the surface of as deposited PZT on GI. Variations in the piezoresponse are clearly visible within a single rosette.

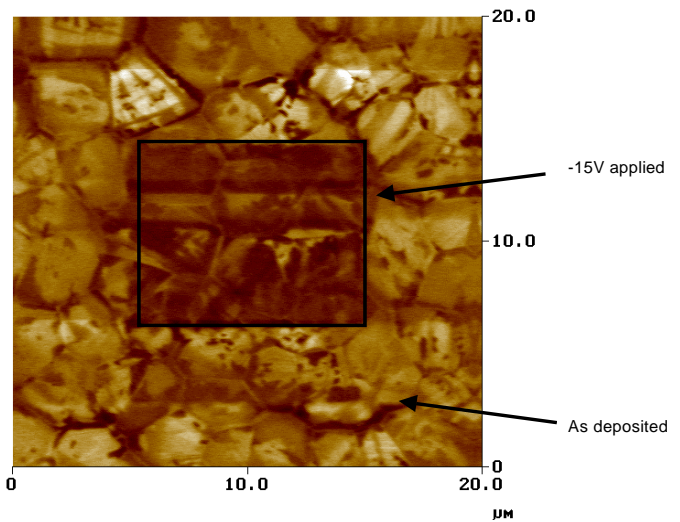


Figure 8: PFM image of fully transformed PZT on GI showing the incomplete poling on application of external electric field.

In the PZT on GI case there is no crystal structure present in the back electrode to impose any orientation in the PZT film. The result of this is that the PZT grows in a random orientation on the ITO. Initial nucleation occurs on surface defects or small regions of crystallinity on the ITO, these regions are not large enough to impose any preferred orientation in the film. Growth of the perovskite phase within the rosette is random with regions of perovskite nucleating from within the rosette in preference to those from the electrode surface<sup>15</sup>. Nucleation of PZT on the Pt

## TRANSFORMATION DEPENDENCE OF PZT AS SHOWN BY PFM

S Dunn and R W Whatmore

electrode produces a film that exhibits very high epitaxy and consists of a number of highly orientated, columnar grains of PZT<sup>16</sup>.

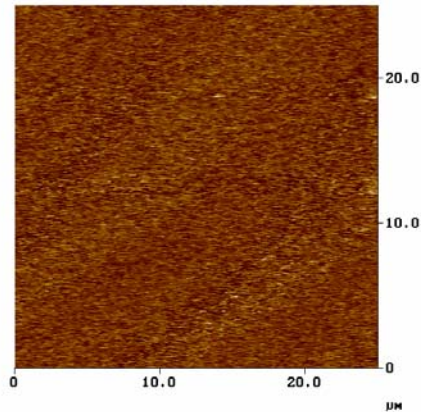


Figure 9: PFM image of PZT grown on STP. The image shows no domain contrast between grains.

### **Conclusions**

Two broad mechanisms for nucleation of perovskite PZT grown by sol-gel methods have been shown to affect the structure of the film. Nucleation due to an interaction with the crystal structure of the electrode produces a film that is orientated whereas nucleation from surface irregularities on a non-crystalline surface produces a film that has no preferred crystal orientation. When the surface of the electrode is rough and crystalline nucleation is restricted to defect regions of the surface and is similar to the case of a non-crystalline surface. However when the surface has some crystal structure the nucleation of the perovskite phase grows in preferred orientations from the initial nucleation point. On a smooth crystalline surface the film grows into columnar grains.

### **Acknowledgements**

The authors would like to thank Dr C Shaw, Dr Q Zhang, Dr P Rayner, Mr A Stallard, The EPSRC, TDK Corporation Japan, The Inamori Foundation and the Royal Academy of Engineering.

### **References**

1. O. Auciello, J. F. Scott and R. Ramesh, The ability of ferroelectric materials to switch robustly from one polarisation state to another forms the basis of a new thin film technology for storing data., *Physics Today*, **51**, 22 (1998)

## TRANSFORMATION DEPENDENCE OF PZT AS SHOWN BY PFM

S Dunn and R W Whatmore

2. Ferroelectric Thin Films VII November 29 - December 3, 1998, Materials Research Society (MRS), Proceedings published electronically, <http://www.mrs.org/meetings/fall98/program/o.html>
3. Ferroelectric Thin Films VIII November 28 - December 2, 1999, Materials Research Society (MRS), Proceedings published electronically, <http://www.mrs.org/meetings/fall99/progbook/ProgramBookY.html>
4. Z. Huang, Q. Zhang and R. W. Whatmore, Journal of Materials Science Letters, **17**, 1157 (1998)
5. Q. Zhang, Z Huang, M. E. Vickers and R. W. Whatmore, Journal of the European Ceramic Society, **19**, 1417 (1999)
6. G. Zavala, J. Fendler and S. Trolier-McKinstry, Journal of Applied Physics, **81**, 7480 (1997)
7. L. M. Eng, M. Abplanalp, P. Gunter and H. J. Guntherodt, Journal of Physics IV France, **8**, Pr9-201, (1998)
8. K. Franke, J. Besold, W. Haessler and C. Seegebarth, Surface Science Letters, **302**, L283 (1994)
9. P. Guthner and K. Dransfield, Applied Physics Letters, **61**, (9), 1137 (1992)
10. T. Hidaka, T. Maruyama, I. Sakai, M. Saitoh, L. A. Wills, R. Hiskes, S. A. Dicarolis, J. Amana and C. M. Foster, Integrated Ferroelectrics, **17**, 319 (1997)
11. S. Dunn and R. W. Whatmore, Journal of Material Science Letters, **20**, 2001, 179-181
12. K. Takada, Journal of Applied Physics, **79**, (1), 134 (1996)
13. S. Dunn and R. W. Whatmore, submitted to European Ceramic Society.
14. R. Wilson, Z. Huang, Q. Zhang, R. W. Whatmore and P. Wang, Integrated Ferroelectrics, **29**, 251 (2000)
15. S. S. Roy, H. Gleeson, C. P. Shaw, R. W. Whatmore, Z. Huang, Q. Zhang and S. Dunn, Integrated Ferroelectrics, **29**, 189 (2000)
16. Z. Huang, Q. Zhang and R. W. Whatmore, Journal of Applied Physics, **86**, No 3, 1662 (1999)